Liberabit, 2025, 31(2), e1085 (julio - diciembre) https://doi.org/10.24265/liberabit.2025.v31n2.1085
ISSN (Digital): 2223-7666

Power spectral analysis of occipital area during eyes-closed and eyes-open

Análisis espectral de potencia en el área occipital durante ojos cerrados y ojos abiertos

Adolfo González-González[a,*], Diego I. Gallardo[b], Yolanda M. Gómez[b], Marc L. Zeise[c]

[a]Departamento de Psicología, Facultad de Humanidades y Educación, Universidad de Atacama, Chile
[b]Departamento de Estadística, Facultad de Ciencias, Universidad del Bío-Bío, Chile
[c]Escuela de Psicología, Facultad de Humanidades, Universidad de Santiago de Chile, Chile

Recibido: 03 de abril de 2025 Aceptado: 05 de junio de 2025

Abstract

Background: Power spectral analysis of the occipital cortex is essential for characterizing brain activity during attentional and relaxed states. **Objectives**: This study aims to develop a predictive model capable of distinguishing between eyes-closed (EC) and eyes-open (EO) states using only two electrodes (O1 and O2), through analysis of power spectral density (PSD) and an interhemispheric asymmetry index. **Method**: EEG recordings from 33 seventh- and eighth-grade students were processed using the Fast Fourier Transform (FFT) and analyzed with a logistic regression model employing a Cauchit link function. **Results**: The model yielded an AUC of 84.2%, with satisfactory precision and sensitivity. While the asymmetry index alone was not highly predictive, it significantly improved performance when combined with frequency-band features. **Conclusions**: This minimal EEG setup demonstrates reliable performance in distinguishing ocular states in non-clinical environments. The approach suggests potential applications in educational and field contexts, emphasizing the value of low-cost EEG solutions in cognitive monitoring.

Keywords: Power spectral analysis, EEG, logistic regression, asymmetry index, FFT.

Resumen

Antecedentes: el análisis espectral de potencia de la corteza occipital es fundamental para caracterizar la actividad cerebral en estados de atención y relajación. **Objetivos**: este estudio tiene como propósito desarrollar un modelo predictivo capaz de distinguir entre los estados de ojos cerrados (EC) y ojos abiertos (EO) utilizando solo dos electrodos (O1 y O2), a partir del análisis de la densidad espectral de potencia (PSD) y un índice de asimetría interhemisférica. **Método**: se procesaron registros de EEG de 33 estudiantes de séptimo y octavo grado mediante la Transformada Rápida de Fourier (FFT), y se analizaron utilizando un modelo de regresión logística con función de enlace tipo Cauchit. **Resultados**: el modelo alcanzó un AUC de 84.2%, con niveles satisfactorios de precisión y sensibilidad. Si bien el índice de asimetría por sí solo no resultó altamente predictivo, su incorporación junto con las bandas de frecuencia mejoró significativamente el rendimiento. **Conclusiones**: esta configuración mínima de EEG demuestra un desempeño confiable para diferenciar estados oculares en entornos no clínicos. El enfoque sugiere aplicaciones potenciales en contextos educativos y de campo, destacando el valor de soluciones EEG de bajo costo para el monitoreo cognitivo.

Palabras clave: análisis espectral de potencia, EEG, regresión logística, índice de asimetría, FFT.

Para citar este artículo:

González-González, A., Gallardo, D. I., Gómez, Y. M., & Zeise, M. L. (2025). Power spectral analysis of occipital area during eyes-closed and eyes-open. *Liberabit, 31*(2), e1085. https://doi.org/10.24265/liberabit.2025.v31n2.1085

* adolfo.gonzalez@uda.cl

Introduction

For a long time, human behavior was understood based on classic behavioural psychology, a positivist paradigm in which only visible and objective behaviour is analyzable. Currently, psychology makes use of tools such as tests and behaviour patterns to establish cognitive processes, intentions and thoughts (Babini et al., 2020; Luck, 2014). These tools have made is possible to establish certain correlates of cognitive and/ or emotional processes with physiological responses (Moodley, 2016). Furthermore, these tools were initially created for medical use, and then have expanded their applications to various fields, including neuropsychology, ergonomics, engineering, etc. (Alagia, 2018; Bonet, 2017; Jahr, 2020; Trejo-Alcantara & Castañeda-Villa, 2017; Vidal & Gatica, 2013).

Electroencephalography (EEG), electrocardiography (ECG), functional near-infrared spectroscopy (fNIRS), and functional magnetic resonance imaging (fMRI) are widely used tools to monitor brain activity (Barret et al., 2020; Phillips et al., 2023). Among them, EEG stands out due to its ability to measure voltage fluctuations across cortical regions with high temporal resolution (Barret et al., 2020). A major advantage of EEG is its non-invasive and painless nature, making it more accessible than fNIRS or fMRI, and more informative for cognitive processes than ECG (Lekova & Chavdarov, 2021; Rhoades & Bell, 2018). The cost-effectiveness and portability of modern EEG systems further enhance their utility in both clinical and non-clinical settings. While various EEG configurations differ in channel count and sampling rate, they all aim to capture precise neural signals. In this study, we focus on detecting eyes-closed (EC) and eyes-open (EO) states–an effect originally described by Berger (1929) and later expanded by Kirschfeld (2005). Our objective is to build a predictive model capable of distinguishing between these ocular states based on EEG-derived features.

This study employs a minimal EEG setup, using only two electrodes (O1 and O2), to distinguish between eyes-open (EO) and eyes-closed (EC) states. In addition to conventional frequency-band segmentation, we introduce the asymmetry index (AI) between these electrodes to enhance interhemispheric analysis and predictive performance. The simplicity of the setup promotes accessibility and cost-effectiveness, making it feasible for non-clinical environments.

Band segmentation enables the capture of neural activity across multiple frequency domains, increasing sensitivity to state-related changes. The inclusion of AI enriches the feature set, offering a complementary dimension to traditional spectral measures. These methods were implemented within the framework of logistic regression using different link functions to optimize classification accuracy.

Previous studies have used more complex systems. For instance, Davis & Kozma (2018) employed 256 electrodes to measure EO/EC differences, reporting changes in theta, low-beta, and high-beta activity across prefrontal and occipital regions. Similarly, Singh et al. (2015) achieved perfect classification (AUC = 1) using 100 single-channel inputs and least-squares support vector machines (LS-SVM). While these models are powerful, their practical implementation is limited due to hardware complexity and cost.

Advances in short-term spectral analysis –such as those described by Alejo-Eleuterio (2022), Fingelkurts & Fingelkurts (2010), Jiménez-Guarneros and Xu et al. (2022)– further support our approach. Segmenting the EEG into 2-second windows, as recommended by Barlow (1985) and Inouye et al. (1991), enhances stability and reduces measurement noise.

More recently, Zhang et al. (2024) demonstrated that reliable distinctions between eyes-open and eyes-closed states can also be achieved using portable EEG devices with a reduced number of electrodes, particularly focusing on alpha-band activity. Their findings support the practical value of minimal EEG configurations in field and applied settings.

This study proposes a predictive model to differentiate between EC and EO states using only two electrodes (O1 and O2), thus facilitating its application in non-clinical settings.

Objective: To establish a logistic regression model capable of predicting eye state (EC vs. EO) based on frequency bands recorded from electrodes O1 and O2, and to assess the contribution of the asymmetry index to this prediction.

Hypotheses: (1) Frequency bands from electrodes O1 and O2 can discriminate between EC and EO states. (2) The asymmetry index enhances the predictive capacity of the model.

This approach contributes to the literature by demonstrating that robust prediction is possible using a minimal number of electrodes, supporting the development of portable and cost-effective solutions for real-time monitoring of cognitive states.

The paper is structured in the following manner. In Section 2, we delve into the theoretical background, providing a concise overview of the statistical tools employed. Moving on to Section 3, we outline the materials and methodology used in our study. Section 4 focuses on the logistic regression applied to address our specific problem, along with the practical implications of the results obtained. Lastly, Section 5 encapsulates the key conclusions drawn from our research, along with suggestions for future investigations.

Theoretical Background

Fast Fourier Transform

Using the Fast Fourier Transform (FFT) (for more details Proakis & Manolakis, 2013), which allows us to calculate the discrete Fourier Transform (DFT), which are often used interchangeably (Cooley et al, 1969) and the DFT can be defined in the following way

$$X_k \sum_{n=0}^{N-1} x_n e^{-\frac{2\pi i}{N} kn}$$

Where $k = 0, \ldots N\text{-}1$. x_k is a discrete aperiodic signal in time, X_k is a set of complex numbers (for more details see Proakis & Manolakis, 2013). In this way, a power spectral density (PSD) decomposition can be obtained, this allows establishing the band of frequencies that are of interest when analyzing the EEG data. Different authors (Davis & Kozma, 2018; Proakis & Manolakis, 2013) have defined the frequency bands in different ranges, in this case, they will be used as shown in Table 1.

Table 1
Frequency Bands Used in the Analysis

Band	Frequencies
δ	≥ .2 – 4
θ	4.0001 – 8
α	8.0001 – 12
β_{low}	12.0001 – 15
β_{middle}	15.0001 – 22
β_{high}	22.0001 – 38
γ	38.0001 – 90
Residual	< .2

Note. Frequency ranges used for FFT band segmentation. *Source*. Own elaboration.

On the other hand, several authors (Hinrikus et al, 2009; Kang et al, 2020) indicate the contribution of the asymmetry index (AI) as a measure of physiological phenomena. For this reason, the following AIs were also carried out for the O1 and O2 electrodes, using the following transformation

$$AI\alpha_o = \frac{\alpha_{O2} - \alpha_{o1}}{\alpha_{O2} + \alpha_{o1}}$$

Where α_{o1} and α_{o2} denote the spectral power in alpha band recorded at electrodes O1 and O2, respectively. This same procedure was carried out for the other frequency bands.

Logistic Regression Model

The logistic regression considers that the response variable (say Y), has a Bernoulli distribution such as

$P(Y_i = 1) = \pi_i$ *and* $P(Y_i = 0) = 1 - \pi_i$, *for* $i = 1,\ldots, n$

Where $\pi_i \in (0,1)$. In our particular problem, $Y_i = 0$ and $Y_i = 1$ represent the eyes-closed (CE) and eyes-open (OE) states, respectively, and π_i denotes the probability of eyes being open. For the case where the population is heterogeneous, a set of $p \geq 1$ observed covariates, say $x_i^\top = (1, x_{i1}, \ldots, x_{ip})$, could be included into the probabilities π_i as

$$g(\pi_i) = \eta_i = x_i^\top \beta = \beta_0 + x_{i1}\beta_1 + \ldots + x_{ip}\beta_p \quad i = 1,\ldots, n$$

Where $\beta = (\beta_0, \ldots, \beta_p)^\top$ is a vector of unknown regression coefficients, η_1 are the linear predictors and $g(\bullet)$: $R \rightarrow (0,1)$ is the link function. For $g(\bullet)$, traditionally the cdf of standard models is used (Hernández & Mazo, 2020; López-González & Ruiz-Soler, 2011; Martínez & Morales, 2001; Pierce & Schafer, 1986). We consider the four cases presented in Table 2 (Koenker & Yoon, 2009). For our particular problem $x_i^\top$ are the DFT for the different bands presented in Table 1 for O1, O2 and IAO.

Table 2
Link Functions Considered for Logistic Regression

Distribution in which is based	link	g(u)
Logistic	logit	log(u/(1 - u))
Normal	probit	$\Phi^{-1}(u)$
Frechet	cloglog	log(-log(1 - u))
Cauchy	cauchit	tan(π_i(u - 1/2))

Note. $\Phi(.)$ and tan denotes the cdf of the standard normal distribution and the tangent function, respectively.

Performance Indexes

AIC and BIC

For comparison purposes, we consider the Akaike information criterion (AIC; Akaike, 1974) and the Bayesian information criterion (BIC; Schwarz, 1978). Such criteria are defined as

$$AIC = -2 \times \log(L) + 2 \times k \quad \textit{and}$$
$$BIC = -2 \times \log(L) + \log(n) \times k$$

where L is the maximum value attached by the likelihood function of the corresponding model, k is the number of parameters and n, is the sample size. The AIC and BIC are statistical measures used to evaluate the fit and complexity of different statistical models. A lower value of AIC or BIC indicates a better fit, with a given penalization for a model with more parameters.

ROC curve

The ROC (Receiver Operating Characteristic) curve is an especially useful graphic representation to establish the efficiency of predictive models with binary variables, slightly varying the cut-off point to carry out the classification (Cerda & Cifuentes, 2012).

The ROC curve allows for establishing the performance of some statistical models in terms of their classification quality. To apply this method, a threshold value must be set (between 0 and 1) that indicates a point where the probability of equal or higher events will be predicted as positive, and less than this threshold, they will be predicted as negative. This allows for establishing a contingency table for that threshold. For the ROC curve, it is required to vary the threshold at all points between 0 and 1 and thus plot the contingency table corresponding to each point. This allows for finding the cut-off point (or threshold) closest to the perfect classification point (.1).

The most used indicator in the analysis of the ROC curve is the area under the curve (AUC), which allows us to interpret the probability that a classifier will score a positive randomly chosen score higher than a negative one.

To understand the ROC curve, it is necessary to understand the contingency tables or confusion matrix. In this case, we can use as an example the Table 3.

Table 3
Confusion Matrix Structure

		Real data		Total
		1	0	
Model outcome	1	True positive (TP)	False positive (FP)	A’
	0	False negative (FN)	True negative (TN)	E’
Total		A	E	

Note. A = Total classified as positive (1), E = Total classified as negative.

Table 3 shows the True Positive (TP) and the True Negatives (TN) are values associated with success within the contingency matrix in the sense that they represent the correctly classified values. In other words, the model predicts as OE, what is OE, and likewise, classifies as CE those who are CE.

An important concept to consider that arises from the above is the true positive ratio (TPR) or success ratio also called «sensitivity», defined by

$$TPR = \frac{TP}{TP + FN}$$

On the other hand, the other value that must be used to establish the graph of a ROC curve is the false positives ratio (FPR) which is given by

$$FPR = \frac{FP}{FP + TN}$$

This concept can be considered the complement of specificity, so that

$$specificity = 1 - FPR$$

The TPR measures whether the diagnostic test or the predictive model is capable of classifying the

positives correctly among all the positives found in the test. While the FPR indicates the number of positive results is incorrect among all negative cases available.

Method

Design

This study uses a pre-experimental within-subject design, in which participants are exposed to two conditions (open eyes and closed eyes) without random assignment or a control group. The objective is to determine whether it is possible to predict eye condition based on the EEG spectral data obtained from occipital electrodes. The analysis also follows a predictive correlational approach, as logistic regression models are used to establish the relationship between frequency band activity and eye state.

Participants

The participants were chosen by convenience sampling. The only exclusion criterion was not having a history of epilepsy or other declared clinical disorders. There is a similar proportion between men and women, as well as between school grades. Specifically, the sample consisted of 33 students: 17 men and 16 women. Among the men, 7 were from 7th grade and 10 from 8th grade, while among the women, 10 were from 7th grade and 6 from 8th grade. The detailed distribution of participants by grade and gender can be observed in Table 4.

Table 4
Distribution of Participants by Grade and Gender

	Grade		Total
	7th	8th	
Men	7	10	17
Women	10	6	16
Total	17	16	33

Note. n = 33. *Source*. Own participant sample.

Instruments

For the recording, the Emotiv Epoc 14-channel EEG model (Emotiv, 2024) was used. This equipment allows the measurement of the O1 and O2 electrodes, as indicated in Figure 1. The location of the electrodes follows a standard and international configuration, most commonly known as the «10-20» method (Klem et al., 1999). In this case, the eye-related effect is expected in the occipital area, which is why only the O1 and O2 electrodes were used to simplify the model.

The equipment was configured to collect 128 measurements per second for each channel (128Hz). Each measurement calculates a value that can be decomposed as a base value of 4200mV, to which differences in electrical potential are added or subtracted.

Figure 1
EEG electrode position scheme

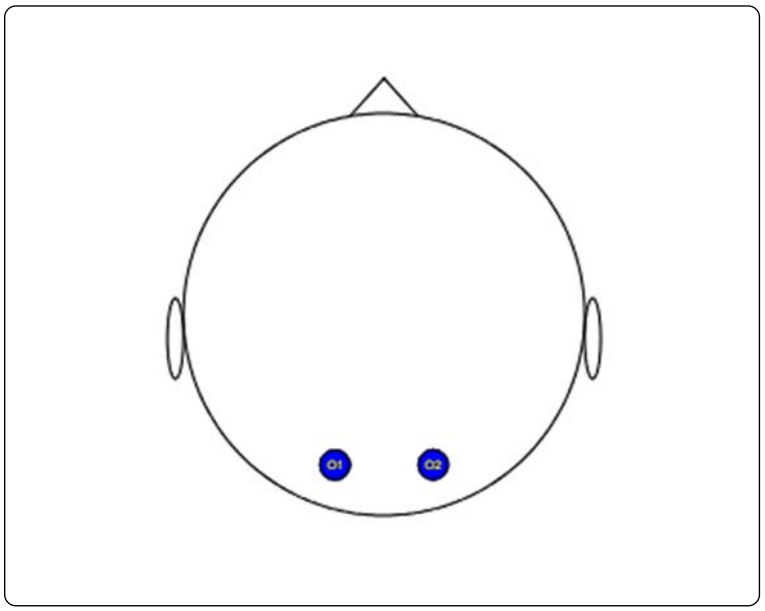

Note. Location of O1 and O2 electrodes according to the 10–20 international system. *Source*. Own elaboration.

Procedure

The procedure followed for data collection involved the following steps:

1. Consent and assent: The participants were informed about the objectives and procedures of the study. Written informed consent was obtained from their tutors, and assent was obtained from each participant, in compliance with ethical standards.
2. Preparation and environment: The recording took place in a room with minimal noise and neutral lighting. Participants were seated comfortably in front of a blank wall to reduce visual distractions.
3. Data collection – open eyes: Participants were instructed to keep their eyes open and look steadily at the blank wall for a period of 5 minutes while the EEG data were recorded continuously.
4. Data collection – closed eyes: Immediately after, participants were instructed to close their eyes and remain still for another 5 minutes while EEG recording continued.
5. Data selection: To ensure data reliability, the middle thirds of each recording period were selected. This approach aimed to allow environmental adaptation and to avoid potential distortions or artifacts that can occur at the beginning or end of the recording sessions. This procedure was based on Jahr (2020).
6. Completion and farewell: At the end of the recording, participants were thanked for their collaboration and given the opportunity to ask any questions before leaving the session.

A general representation of the procedure can be observed in Figure 2.

Data analysis

Data preprocessing included the application of a minimum frequency filter of 0.4Hz and a high-frequency filter of 90Hz. Segments of 10 seconds (1280 measurements), without overlap, were extracted. FFT was applied to each segment to compute the power spectral density and extract average amplitude values for each frequency band (as per Table 1). These values were then used to compute asymmetry indices (Equation 2), followed by feature selection and logistic regression modeling.

Model selection was based on AUC, AIC, and BIC indicators. The final model was trained on a random 70% of the data.

In total, we collected 933,557 measures, corresponding to approximately 50% for each condition studied (463,416 for CE and 470,141 for OE). The analysis was performed using R software (R Core Team, 2021), with the eegkit package (Helwig, 2018).

Figure 2
EEG Processing Pipeline

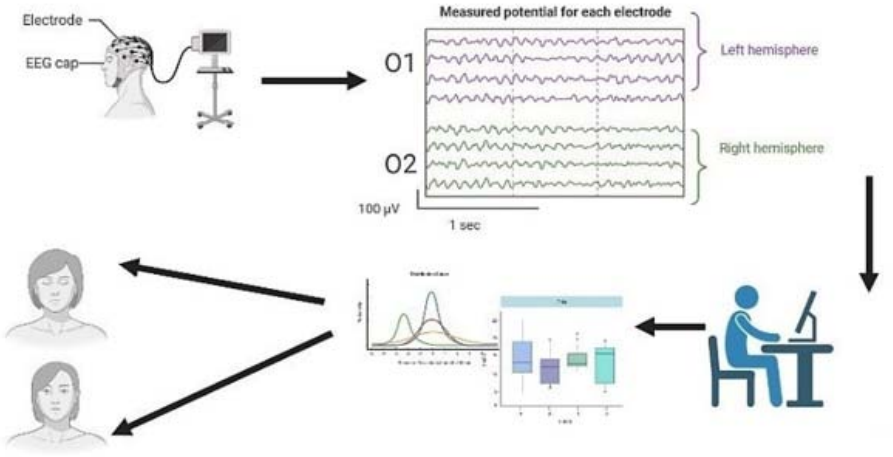

Note. Diagram of the sequential steps from acquisition to prediction. *Source*. Own elaboration.

Results

The data extracted from the Emotiv software were organized based on each frequency band per electrode, along with the asymmetry index (AI) of each band.

Table 5 summarizes the AUC, AIC, and BIC for four link functions (logit, probit, cloglog, and cauchit).

From the table, it can be observed that the cauchit link function displays the lowest AIC and BIC values, indicating a better fit for the data. Additionally, the cauchit link function also exhibits the highest AUC, suggesting better predictive performance. Due to these reasons, we will focus on utilizing the cauchit link function for further analysis.

Table 5
Model Fit Indices by Link Function

	logit	probit	cloglog	cauchit
AUC	.836	.832	.812	.842
AIC	554.8	556.9	576.6	545.7
BIC	648.0	650.0	669.8	638.8

Notes. AUC = Area Under Curve, AIC = Akaike Information Criterion, BIC = Bayesian. Information Criterion.

The logistic regression analysis with a cauchit link yielded significant estimates for each band, as well as the asymmetry index, across both electrodes. However, the contributing predictors varied across electrodes, in Table 6.

Table 6
Regression Coefficients by Frequency Band and Electrode

Electrode	Band	Estimate	Pr (> |z|)
(Intercept)		-.7103	.1384
O1	δ	1.4225	.0112*
	θ	-.5666	.6713
	α	-.4745	.9104
	β_{low}	-8.5399	.1770
	β_{middle}	2.3335	.7658
	β_{high}	12.0903	.3305
	γ	-51.0291	.0070**
O2	δ	-.5654	.3213
	θ	-1.5383	.1247
	α	-4.9096	.1565
	β_{low}	13.2459	.0175*
	β_{middle}	8.4424	.2106
	β_{high}	-104363	.3396
	γ	16.6073	.2647
IAO	δ	2.1005	.3638
	θ	9.1618	.0090**
	α	2.7333	.5812
	β_{low}	-8.33077	.1155
	β_{middle}	-12.6224	.0251*
	β_{high}	1.4888	.4660
	γ	-1.8823	.0802.

*Notes. *p < .05, **p < .01. Non-significant values omitted.*

Importantly, the theta, low-beta, and high-beta bands showed significant predictive power for O1, while different bands were relevant for O2 and the AI. These findings partially confirm the first hypothesis, indicating that frequency bands from O1 and O2 are indeed useful in distinguishing EC and EO states.

The AI alone was not consistently significant across all bands, but its combination with other variables contributed positively to model performance. This offers partial support for the second hypothesis, which proposed that the asymmetry index would enhance prediction.

Figure 3
Receiver Operating Characteristic (ROC) Curve

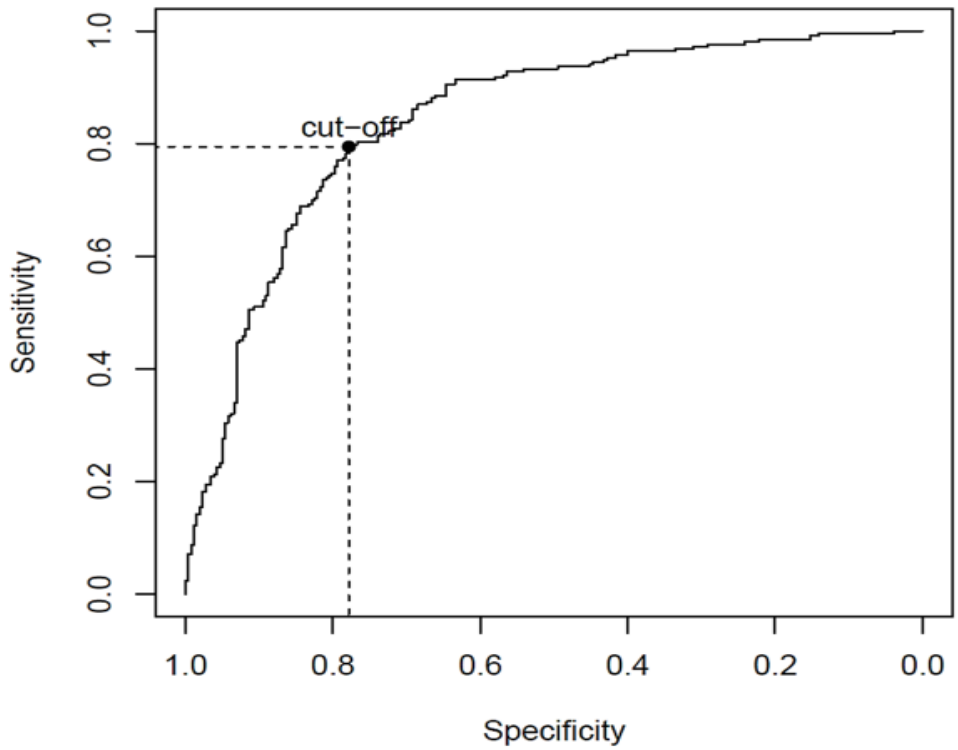

Note. Represents model sensitivity and specificity across cut-off thresholds.

Figure 3 shows the ROC curve for the model, confirming its classification quality. The optimal cut-off point (.653) balances sensitivity (.794) and specificity (.778), as detailed in Table 7.

Table 8 reports precision and error metrics for both training and testing datasets. The average accuracy in testing was 66.7%, with an F-measure of .684, suggesting moderate generalizability. While slightly lower than training accuracy, the consistency between training and test performance supports the model's stability.

This indicates that the model is performing reasonably well in predicting the target variable. The AUC value of 84.2% suggest that the model has good discriminative power in distinguishing between positive and negative instances. Finally, Table 9 shows the confusion matrix used to assess prediction outcomes. The model correctly identified 79.4% of EC and

77.8% of EO cases, which aligns with the model's AUC and supports its utility in real-time EC/EO classification using only two electrodes.

Overall, these evaluation metrics suggest that the model is performing well in terms of both its ability to identify positive instances and its ability to correctly classify negative instances.

Table 7
ROC Curve Performance Measures

Optimal cut-off point	Sensitivity	Specificity
.653	.794	.778

Note. Includes sensitivity and specificity at optimal cut-off point.

Table 8
Classification Metrics for Training and Testing Sets

Indicator	Training	Testing
Average accuracy	.786	.667
F-Measure	.786	.684
MAE	.214	.333
RMAE	.462	.578
Precision	.794	.627
Recall	.778	.752

Notes. MAE = Mean Absolute Error, RMAE = Root Mean Absolute Error.

Table 9
Prediction Outcomes by Real State

		Real state		Real state	
		0	1	0	1
Prediction	0	77.8%	20.6%	75.2%	41.2%
	1	22.2%	79.4%	24.8%	58.8%
		Training		Testing	

Note. Percentages of correctly classified observations in training and testing sets.

Discussion

The results of this study support the viability of using only two occipital electrodes (O1 and O2) to predict eyes-closed (EC) and eyes-open (EO) states through power spectral analysis and logistic regression. The achieved AUC of 84.2% suggests that the model has a strong discriminative capacity, reinforcing the relevance of low-cost, non-invasive EEG setups in cognitive state monitoring.

Regarding the hypotheses, the first is supported by the results: frequency bands from O1 and O2 electrodes provided statistically significant predictors for distinguishing EC and EO states. Specifically, different frequency bands contributed to the model depending on the electrode, consistent with previous findings on localized occipital activity.

The second hypothesis was partially supported: while the asymmetry index (AI) alone did not reach high predictive accuracy (AUC < 65%), it enhanced model performance when used alongside frequency bands, indicating its utility as a complementary feature.

Compared to previous works using large arrays of electrodes (e.g., Davis & Kozma., 2018; Ma & Gao, 2020; Singh et al., 2015), the current model demonstrates that similar levels of performance can be approached with a drastically simplified setup. This has significant practical implications, especially for real-time monitoring in field settings, educational environments, or low-resource contexts.

Several limitations must be acknowledged. The sample size was relatively small (n = 33) and limited to a narrow age range (middle school students), which may constrain the generalizability of the results. Additionally, the absence of electrodes in frontal or parietal regions might overlook other relevant neural signatures. Future studies should explore the generalization of this model across broader populations and test the integration of additional physiological or behavioral variables.

Conclusion

In line with this, recent research by Metzen et al. (2022) examined the short-term reliability of alpha-band asymmetry across frontal and parietal regions using different EEG systems. Their findings emphasize the importance of regional differences in alpha asymmetry and the methodological challenges of achieving consistent measurements across devices. This supports the relevance of exploring regional contributions beyond the occipital cortex in future work.

In conclusion, this study demonstrates that a simple EEG configuration combined with appropriate spectral and statistical processing can effectively distinguish basic attentional states. These findings contribute to the development of accessible EEG-based monitoring tools and support the continued refinement of predictive models using minimal neural data.

Future research should aim to validate these findings in more diverse samples, compare the performance across different EEG headsets, and explore applications beyond ocular states, such as emotional or cognitive workload detection.

Conflict of interest

The authors declare that there is no conflict of interest regarding the publication of this paper.

Ethical responsibility

The data ser used in this experiment is collected by Isabel Jahr from Chile in the frame of the project DICYT 031693Z given to Marc L. Zeise from the University of Santiago de Chile. The ethical safeguards have been applied by an authorized committee of the same university. For more information contact the corresponding author.

Authorship contributions

AGG: Research conceptualization, data processing and analysis, visualization of results and drafting of the manuscript.

DIG: Research conceptualization, data processing and analysis, and manuscript writing.

YMG: Research conceptualization, data processing and analysis, and manuscript writing.

MLZ: Data collection and revision of the manuscript.

References

Akaike, H. (1974). A new look at the statistical model identification. *IEEE Transactions on Automatic Control*, *19*(6), 716-723. https://doi.org/10.1109/tac.1974.1100705

Alagia, R. A. (2018). *Procesamiento de artefactos en EEG para aplicaciones de comunicación y control* [Trabajo de fin de grado, Universitat Politècnica de València]. Repositorio UPV. http://hdl.handle.net/10251/104163

Babini, M., Kulish, V., & Namazi, H. (2020). Physiological state and learning ability of students in normal and virtual reality conditions: Complexity-based analysis. *Journal of Medical Internet Research*, *22*(6), e17945. https://doi.org/10.2196/17945

Barlow, J. S. (1985). A general-purpose automatic multichannel electronic switch for EEG artifact elimination. *Electroencephalography and Clinical Neurophysiology, 60*(2), 174-176. https://doi.org/10.1016/0013-4694(85)90025-2

Barrett, K. E., Barman, S. M., Brooks, H., &, Yuan J. (2020). *Ganong fisiología médica* (26.ª ed.). McGraw-Hill Interamericana.

Berger, H. (1929). *Über das Elektrenkephalogramm des Menschen*. *Archiv für Psychiatrie und Nervenkrankheiten*, *87*, 527-570. https://doi.org/10.1007/BF01797193

Bonet, J. (2017). *Visualización de valencia (Pleasure-Dominance-Arousal) en el dispositivo MUSE* [Tesis de maestría, Universitat de Lleida]. http://hdl.handle.net/10459.1/60050

Cerda, J., & Cifuentes, L. (2012). Uso de curvas ROC en investigación clínica: Aspectos teórico-prácticos. *Revista Chilena de Infectología*, *29*(2), 138-141. https://doi.org/10.4067/S0716-10182012000200003

Cooley, J., Lewis, P., & Welch, P. (1969). The finite Fourier transform. *IEEE Transactions on Audio and Electroacoustics*, *17*(2), 77-85. https://doi.org/10.1109/TAU.1969.1162036

Davis, J. J. J., & Kozma, R. (2018). Visualization of human cognitive state monitored by high-density EEG arrays. *Procedia Computer Science*, *144*, 219-231. https://doi.org/10.1016/j.procs.2018.10.522

EMOTIV. (2024). *EPOC X - 14 channel wireless EEG headset*. http://www.emotiv.com/epoc/

Fingelkurts, A. A., & Fingelkurts, A. A. (2010). Morphology and dynamic repertoire of EEG short-term spectral patterns in rest: Explorative study. *Neuroscience Research*, *66*(3), 299-312. https://doi.org/10.1016/j.neures.2009.11.014

Helwig, N. (2018) eegkit: Toolkit for Electroencephalography Data. R package version 1.0-4. Available online: https://CRAN.R-project.org/package=eegkit

Hernández, F., & Mazo, M. (2020). Modelos de Regresión con R. Available on https://fhernanb.github.io/libro regresion.

Hinrikus, H., Suhhova, A., Bachmann, M., Aadamsoo, K., Võhma, Ü., Lass, J., & Tuulik, V. (2009). Electroencephalographic spectral asymmetry index for detection of depression. *Medical & Biological Engineering & Computing*, *47*(12), 1291-1299. https://doi.org/10.1007/s11517-009-0554-9

Inouye, T., Shinosaki, K., Sakamoto, H., Toi, S., Ukai, S., Iyama, A., Katsuda, Y., & Hirano, M. (1991). Quantification of EEG irregularity by use of the entropy of the power spectrum. *Electroencephalography and Clinical Neurophysiology, 79*(3), 204-210. https://doi.org/10.1016/0013-4694(91)90138-t

Jahr, M. (2020). *Evaluación de un biomarcador como indicador de Trastorno de Déficit de Atención/Hiperactividad (TDAH): Un estudio correlacional* [Tesis de maestría, Universidad de Santiago de Chile].

Jiménez-Guarneros, M., & Alejo-Eleuterio, R. (2022). A class-incremental learning method based on preserving the learned feature space for EEG-based emotion recognition. *Mathematics*, *10*(4), 598. https://doi.org/10.3390/math10040598

Kang, M., Kwon, H., Park, J. H., Kang, S., & Lee, Y. (2020). Deep-asymmetry: Asymmetry matrix image for deep learning method in pre-screening depression. *Sensors*, *20*(22), 6526. https://doi.org/10.3390/s20226526

Kirschfeld, K. (2005). The physical basis of alpha waves in the electroencephalogram and the origin of the «Berger effect». *Biological Cybernetics*, *92*(3), 177-185.https://doi.org/10.1007/s00422-005-0547-1

Klem, G. H., Lüders, H. O., Jasper, H. H., & Elger, C. (1999). The ten-twenty electrode system of the International Federation. *Electroencephalography and Clinical Neurophysiology Supplement*, *52*, 3-6.

Koenker, R., & Yoon, J. (2009). Parametric links for binary choice models: A Fisherian-Bayesian colloquy. *Journal of Econometrics*, *152*(2), 120-130. https://doi.org/10.1016/j.jeconom.2009.01.009

Lekova, A., & Chavdarov, I. (2021). A fuzzy shell for developing an interpretable BCI based on the spatiotemporal dynamics of the evoked oscillations. *Computational Intelligence and Neuroscience*, *2021*(1). https://doi.org/10.1155/2021/6685672

López-González, E., & Ruiz-Soler, M. (2011) Análisis de datos con el Modelo Lineal Generalizado. Una Aplicación con R. *Revista española de pedagogía*, *248*, 59-80.

Luck, S. J. (2014). *An introduction to the event-related potential technique* (2nd ed.). MIT Press. https://mitpress.mit.edu/9780262525855/an-introduction-to-the-event-related-potential-technique/

Ma, P., & Gao, Q. (2020). EEG signal and feature interaction modeling-based eye behavior prediction research. *Computational and Mathematical Methods in Medicine*, *2020*(1). https://doi.org/10.1155/2020/2801015

Martínez, M. A., & Morales, J. (2001). *Modelos lineales generalizados*. Universidad Miguel Hernández de Elche. https://tauniversity.org/sites/default/files/modelos_lineales_generalizados_book_pdf.pdf

Metzen, D., Genç, E., Getzmann., Larra, F., Wascher, E., & Ocklenburg, S. (2022). Frontal and parietal EEG alpha asymmetry: A large-scale investigation of short-term reliability on distinct EEG systems. *Brain Structure Function*, *227*, 725-740. https://doi.org/10.1007/s00429-021-02399-1

Moodley, A. (2016). Understanding vision and the brain. *Community Eye Health*, *29*(96), 61-63.

Phillips, V. Z., Canoy, R. J., Paik, S. H., Lee, S. H., & Kim, B. M. (2023). Functional near-infrared spectroscopy as a personalized digital healthcare tool for brain monitoring. *Journal of Clinical Neurology*, *19*(2), 115-124. https://doi.org/10.3988/jcn.2022.0406

Pierce, D. & Schafer, D. (1986). Residuals in Generalized Linear Models. Journal of the American Statistical Association, 81, 977-986.

Proakis, J., & Manolakis, D. (2013). *Digital signal processing* (4th ed.). Pearson International.

Rhoades, R., & Bell, D. (2018). *Fisiología médica. Fundamentos de medicina clínica* (5.ª ed.). Wolters Kluwer.

Singh, P., Joshi, S. D., Patney, R. K., & Saha, K. (2015). Fourier-based feature extraction for classification of EEG signals using EEG rhythms. *Circuits, Systems, and Signal Processing*, *35*(10), 3700-3715. https://doi.org/10.1007/s00034-015-0225-z

Schwarz, G. (1978). Estimating the Dimension of a Model. *The Annals of Statistics*, *6*(2), 461-64. http://www.jstor.org/stable/2958889.

Trejo-Alcantara, G., & Castañeda-Villa, N. (2017). Effect of EEG pre-processing on independent component analysis: Reduction of cochlear implant artifact in auditory evoked potentials. *Revista Mexicana de Ingeniería Biomédica*, *38*(1), 382-389. https://doi.org/10.17488/rmib.38.1.34

Vidal, C., & Gatica, V. (2013). Design and implementation of a digital electrocardiographic system. *Revista Facultad de Ingeniería Universidad de Antioquia*, *55*, 99-107. https://doi.org/10.17533/udea.redin.14718

Xu, B., Li, W., Liu, D., Zhang, K., Miao, M., Xu, G., & Song, A. (2022). Continuous hybrid BCI control for robotic arm using noninvasive electroencephalogram, computer vision, and eye tracking. *Mathematics*, *10*(4), 618. https://doi.org/10.3390/math10040618

Zhang, Y., Zhang, Z., Du, F., Song, J., Huang, S., Mao, J., Xiang, W., Wang, F., Liang, Y., Chen, W., Lin, Y., & Han, C. (2024). Shared oscillatory mechanisms of alpha-band activity in prefrontal regions in eyes open and closed state using a portable EEG acquisition device. *Scientific Reports, 14(1)*, 26719. https://doi.org/10.1038/s41598-024-78173-0

Adolfo González-González

Departamento de Psicología, Facultad de Humanidades y Educación, Universidad de Atacama, Chile.

Adolfo González-González es psicólogo por la Universidad de Santiago de Chile, con magíster en Psicología Educacional en la misma institución y magíster en Estadística por la Universidad de Atacama. Su labor académica y de investigación se centra en neurociencias, psicología educacional y metodología cuantitativa, con experiencia en análisis de datos y modelamiento estadístico aplicado a la psicología. Ha participado en múltiples investigaciones y congresos nacionales e internacionales, contribuyendo al estudio de biomarcadores en salud mental y factores psicosociales en educación.

ORCID: https://orcid.org/0000-0001-8566-628X

Corresponding author: adolfo.gonzalez@uda.cl

Diego I. Gallardo

Departamento de Estadística, Facultad de Ciencias, Universidad del Bío-Bío, Concepción, Chile.

Diego Gallardo es académico en el Departamento de Estadística de la Universidad del Bío-Bío, Chile. Obtuvo su grado de doctor en Estadística en la Universidad de São Paulo en 2014 y su licenciatura en Estadística y Computación en 2009 en la Universidad de Santiago de Chile. Fue editor ejecutivo de la *Chilean Journal Of Statistics* y es mantenedor de los siguientes paquetes en R: skewMLRM, tpn, extrafrail, MCPModBC, PScr y RBE3.

ORCID: https://orcid.org/0000-0001-8184-7403

dgallardo@ubiobio.cl

Yolanda M. Gómez

Departamento de Estadística, Facultad de Ciencias, Universidad del Bío-Bío, Concepción, Chile.

Yolanda Gómez es una científica, investigadora y académica chilena. Es reconocida por sus trabajos sobre modelos de sobrevivencia con fracción de cura, teoría de distribuciones y modelos de regresión. Ha sido distinguida por el Ministerio de Ciencia, Tecnología, Conocimiento e Innovación de Chile como una de las mujeres referentes en ciencia, tecnología, conocimiento e innovación (CTCI) de Chile. Fue directora y presidenta de la Sociedad Chilena de Estadística.

ORCID: https://orcid.org/0000-0002-8092-9666

ygomez@ubiobio.cl

Marc L. Zeise

Escuela de Psicología, Facultad de Humanidades, Universidad de Santiago de Chile, Santiago, Chile.

Marc Zeise, neurobiólogo alemán con destacada trayectoria académica e investigativa, ha sido profesor titular en la Universidad de Chile, en la Facultad de Humanidades, Escuela de Psicología, donde también se desempeñó como coordinador de Áreas Básicas hasta 2023. Está titulado como biólogo en la Universidad de Múnich y obtuvo su doctorado en Ciencias en la Universidad de Bochum, Alemania. Posteriormente, logró un segundo doctorado de habilitación en la Universidad de Múnich, lo que le otorgó la *venia legendi*, calificándolo para ejercer como profesor titular en actividad científica.

ORCID: https://orcid.org/0000-0001-7683-4878

marc.zeise@usach.cl